

**UNCLASSIFIED**  
**AD**

**207 094**

FOR  
MICRO-CARD  
CONTROL ONLY

**1 OF 1**

Reproduced by

**Armed Services Technical Information Agency**

**ARLINGTON HALL STATION; ARLINGTON 12 VIRGINIA**

**UNCLASSIFIED**

"NOTICE: When Government or other drawings, specifications or other data are used for any purpose other than in connection with a definitely related Government procurement operation, the U.S. Government thereby incurs no responsibility, nor any obligation whatsoever; and the fact that the Government may have formulated, furnished, or in any way supplied the said drawings, specifications or other data is not to be regarded by implication or otherwise as in any manner licensing the holder or any other person or corporation, or conveying any rights or permission to manufacture, use or sell any patented invention that may in any way be related thereto."

AD No. 207094

ASTIA FILE COPY

PICATINNY ARSENAL  
DOVER, NEW JERSEY



FELTMAN  
RESEARCH AND ENGINEERING  
LABORATORIES

FC  
BAC

MISSILE WARHEAD AND SPECIAL PROJECTS LABORATORY

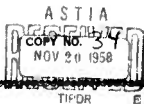
ANALYTICAL SECTION

TECHNICAL MEMORANDUM  
NO. 127A53

MEAN PRESENTED AREA OF SMALL STEEL  
FRAGMENTS MEASURED BY MEANS OF  
FREE FALL IN A VISCOUS FLUID

BY  
I. H. STEIN

OCTOBER 1958



MISSILE WARHEAD & SPECIAL PROJECTS LABORATORY

ANALYTICAL SECTION

Technical Memorandum No. 127A53

MEAN PRESENTED AREA OF SMALL STEEL FRAGMENTS MEASURED  
BY MEANS OF FREE FALL IN A VISCOUS FLUID

By:

I. H. STEIN

Approved by:

*B. Karin*

B. KARIN

Chief, Analytical Section

*V. Lindner*

V. LINDNER

Chief, Missile Warhead &  
Special Projects Lab

October 1958

### ABSTRACT

✓ The mean presented areas of small irregular shaped steel fragments, within and beyond the lower limit of the icosahedron gage, were measured by a new method. This technique, based upon the free fall of a fragment in a viscous fluid and the fragment weight, yields results comparable in accuracy to the icosahedron gage; an average deviation of 4.3% and a maximum deviation of 10% from true values were observed. For fragments below 30 grains, an empirical expression for presented area was determined, as follows:

$$\bar{A} = \frac{W}{K_1 V + K_2}$$

where

- $\bar{A}$  = Mean presented area, taken in the manner of the current literature as  $\frac{1}{4}$  of the total surface area (sq. cms.).
- W = Weight of fragment (grams).
- V = Terminal velocity of fragment (cms./sec).
- $K_1$  &  $K_2$  = Constants depending upon the fluid density, viscosity, and temperature.  $K_1$  &  $K_2$  = .0756 and .4700 for liquid methyl silicone fluid (Dow-Corning 200 Fluid, density 0.971 gms/cc<sup>3</sup> at 25° C, kinematic viscosity, 200 centistokes at 25° C, and test temperature of 25° C  $\pm$  2° C).
- The expression above holds for chunky fragments with no major concave contour.

#### ACKNOWLEDGEMENT

The idea for measurement of fragment presented area by fall in a viscous fluid was generated by Mr. E. Fairbanks of Technical Laboratory Services, FREL, Picatinny Arsenal, and is reported in Reference 6. The author wishes to express his appreciation to Mr. Fairbanks, and his associate, Mr. R. McCloud, for their assistance in connection with the work reported herein.

# TABLE OF CONTENTS

	<u>Page</u> <u>No.</u>
Abstract	1
Acknowledgement	11
Table of Contents	111
Conclusion	1
Introduction	2
Summary of Results	4
Experimental Procedure	5
Discussion	8
Appendix	
Applicability of Stokes Law to the Measurement of Sphere Radius	25-29
References	30
Distribution List	31-32

### CONCLUSIONS

For steel fragments below 30 grain weight, mean presented areas can be measured with simple equipment in a reasonable time. An average deviation of 4.3% and a maximum deviation of 10% was achieved in this measurement for chunky fragments with no major concave contours.

These results were obtained with 32 fragments including:

- a. Random shaped steel shell fragments previously measured on the icosahedron gage at B. R. L. (13.5 to 32 grains).
- b. Steel parallelepipeds, cylinders, and spheres (0.32 to 54 grains).
- c. Brass cylinders (0.97 to 5.1 grains)

Data obtained indicated that the mean presented area (as defined below) of random shaped steel fragments under 30 grains subscribe to the following empirical expression:

$$\bar{A} = \frac{W}{K_1 \bar{V} + K_2} \quad \text{Equation (1)}$$

where:  $\bar{A}$  - Mean presented area or  $\frac{1}{2}$  of the total surface area, in the manner of the current literature (sq. cms.).

W - fragment weight (grams).

$\bar{V}$  - Terminal velocity of fragment (cms./sec.).

$K_1$  &  $K_2$  - .0758 and .4700 for liquid methyl silicone fluid (Dow-Corning 200 fluid, density, 0.971 gms/cm<sup>3</sup> at 25°C, kinematic viscosity, 200 centistokes at 25°C, and ambient temperature of 25°C  $\pm$  2°C).



### INTRODUCTION

In the pursuance of weapons lethality forecasts, the mean presented area of a random shaped fragment in free flight appears as a significant determining value.

The expression for the drag force producing a negative acceleration on the fragment is as follows:

$$-ma = Cd A \rho V^2$$

where:

$a$  = acceleration

$m$  = mass

$A$  = presented area

$\rho$  = air density

$V$  = velocity

$Cd$  = coefficient of drag

The mean presented area ( $\bar{A}$ ), can be shown to be equal to one-fourth of the surface area of the fragment. Hereafter, the mean presented area may be referred to simply as  $\bar{A}$ .

Before the advent of the icosaedron gage in 1953, the measurement of the  $\bar{A}$  of a fragment was an extremely laborious lengthy task involving a great many readings. B.R.L. Report No. 877 states that the icosaedron gage could make a measurement in less than one hour with an overall instrument error of  $\pm 5\%$  and was limited to fragments above .023 sq. in. for  $\bar{A}$ . The method of this report makes possible the measurement of small fragments with no observed lower limit in  $\bar{A}$  and in the comparatively short time of ten minutes or less.

Mr. Bernard Fairbanks in his Instrumentation Report No. TR-360-58/1 dated June 12, 1958, "Determining the Presented Area of a Fragment from its Terminal Velocity in a Gresss Column", suggested the use of the terminal velocity in viscous silicone fluid and developed an empirical equation for  $\bar{A}$  of spheres of different sizes.

The subject of this report extends the method of free fall through a fluid for the determination of mean presented area to shapes other than spheres, i.e., to other regular shapes and to the practical case of small random shaped fragments.

### SUMMARY OF RESULTS

Various regular shaped fragments such as spheres, cylinders, and rectangular parallelepipeds along with irregular fragments were measured with the following results:

<u>Fragment Material &amp; Shape</u>	<u>No. of Fragments Tested</u>	<u>Method Used</u>	<u>Weight Range Grains</u>	<u>*<math>\bar{A}</math> Range Sq. CM</u>	<u><math>\bar{A}</math> Average % Deviation From True Value</u>
Steel Spheres	4	Equation (1)	.84-54	.045-.70	5.5
Steel Rod	7	" (1)	.32- 6.2	.033-.24	3.8
Steel Square	7	" (1)	1.0 -18.5	.075-.55	5.4
Steel Shell Fragments	8	" (1)	13.5 -32.3	.48-1.48	4.6
Brass Cylinders	5	" (1)	.98- 5.2	.053-.21	2.6
Copper Sphere	1	" (1)	4.137	.117	1.4
Steel Spheres	4	" (3)	.84-54.	.045-.70	6.3
Steel Spheres	4	" (4)	.84-54.	.045-70	2.0
Aluminum Cylinders	5	" (5)	.41-2.0	.067-.232	0.4

The  $\bar{A}$  for regular shaped fragments, calculated from the terminal velocity measurement and equation (1), were compared to the values given by  $\frac{1}{2}$  the total surface area.

The  $\bar{A}$  for the irregular shell fragments, calculated from the terminal velocity measurement and equation (1), were compared to the values received from Mr. M. Famiglietti of the Ballistic Research Laboratories.

An average deviation of 4.3% for 32 determinations was achieved in using equation (1).

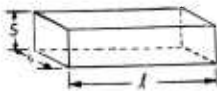
\*  $\bar{A}$  = Mean presented area

### EXPERIMENTAL PROCEDURE

For the accumulation and analysis of data so that an empirical relationship could be found to measure  $\bar{A}$ , regular shaped steel cylinders and rectangular parallelepipeds were fabricated. These were made to the specification that the shape ratio of maximum regular to minimum regular dimension be within the limit of  $\frac{1}{2}$  to 5 and that the weights range below 25 grains. For cylinders, the shape ratio was taken as the length to diameter, while for square cross sectioned parallelepipeds, the shape ratio was taken as length to one side of the square of cross section as illustrated:



$$\text{Shape ratio} = \frac{l}{d}$$

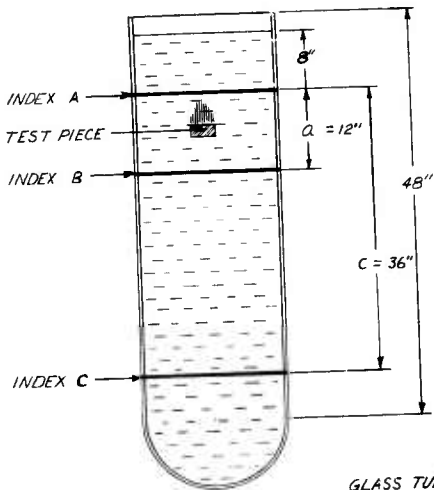


$$\text{Shape ratio} = \frac{l}{s}$$

These regular shaped pieces were dropped in Dow Corning 200 fluid, contained in the four foot glass tube as shown in Figure 1, and terminal velocity was calculated.

The Dow Corning 200 fluid used had a density of 0.971 and a kinematic viscosity of 200 centistokes at 25°C. The ambient temperature in the air conditioned room was 25°C  $\pm$  2°C.

The particle terminal velocity was calculated from the time of fall through 36". The time was the average of four individual falls. Orientation of the particle before drop did not affect the measured time and the particle



GLASS TUBE

I.D = 1.465

O.D = 1.613

TEST CONTAINER SETUP FOR FRAGMENT TERMINAL  
VELOCITY IN A VISCOUS FLUID

FIG. 1

always took the same preferred orientation in the fluid on reaching terminal velocity.

A test for terminal velocity was that the time of travel for the first 12" or 36" travel equal  $1/3$  of the total time for 36". This condition was met by allowing an 8 inch fall before initiating velocity timing as shown on sketch of glass tube.

Time was measured with a hand operated stop watch No. 144 made by Minerva of Switzerland, graduated in  $1/10$ th of a second. The watch was started and stopped at the indices signifying the beginning of the "a" interval and the end of the "o" interval as these indices were crossed by the falling fragment.

Before being dropped in the Dow Corning silicone fluid the particles were weighed with a chemical balance and measured for all significant dimensions with a micrometer.

After drawing various curves, the ratio of weight to mean presented area was plotted against terminal velocity, using the data for cylinders, rectangular parallelepipeds, and the data for spheres from Reference 6. A mathematical expression for mean presented area was derived from this graph. To test this expression, irregular shell fragments, previously measured by the Ballistic Research Laboratories, were remeasured using the method of this report. Likewise, spheres and cylinders of metals other than steel were used to check the validity of this method.

### DISCUSSION

The evolution of a measurement method for obtaining mean presented area of an irregular shaped fragment h.w.e. by the very nature of the problem, involved a succession of lengthy and intricate approaches, each attempting to increase the reliability of the measurement and decrease the excessive time and labor required.\*

The lecohedron gage as described in B.R.L. Report No. 877 represents the culmination of previous efforts and is the current instrument used. B.R.L. Report No. 877 states that measurement of a fragment can be made in less than an hour with a  $\pm 5\%$  overall instrument error, and the range of mean presented area measurable by the instrument is .023 in<sup>2</sup> to 5 in.<sup>2</sup>

B. Fairbanks, in his report on spheres dropped in a viscous fluid (Reference 6), took a distinctly different tack for the problem, arriving at an empirical expression. At the outset of the present investigation, an attempt was made to correlate the experimental terminal velocities for spheres from the report of B. Fairbanks with Stokes law for small spheres falling in a viscous fluid, namely: 
$$V = \frac{2g r^2 (d_1 - d_2)}{9\eta}$$

where:

V = terminal velocity of a sphere falling in a fluid

g = acceleration of gravity

r = radius of the sphere

d<sub>1</sub> = density of small sphere

\* Some of these approaches are presented in Ballistic Research Laboratories Report Nos. 877 and 501 listed in the "References".

$d_2$  = density of fluid

$n$  = coefficient of viscosity of fluid

\*The dimensions for spheres of different diameters, calculated from Stokes law, differed from the actual dimensions as shown in Table I and Figures Nos. 2 and 3. Since the radius squared was used in both the computing of actual sphere presented area and the Stokes equation, the correlation between actual radius and Stokes law calculated radius was based on the radius squared as follows:

1. Plotting  $r_{\text{Stokes}}^2$  against  $R^2$  actual on logarithmic paper and achieving a straight line, the equation

$$R^2 \text{ actual} = 7.42 (r_{\text{Stokes}}^2)^{1.41} \quad \text{Equation (3)}$$

was derived. The average deviation for  $\bar{A}$  using equation (3) above was 6.3%.

2. A second correlation was worked out by inductive reasoning from the available data. Examination of the data pointed to an exponential relationship with a decreasing exponent as  $r_{\text{Stokes}}^2$  increased, resulting in the following expression:

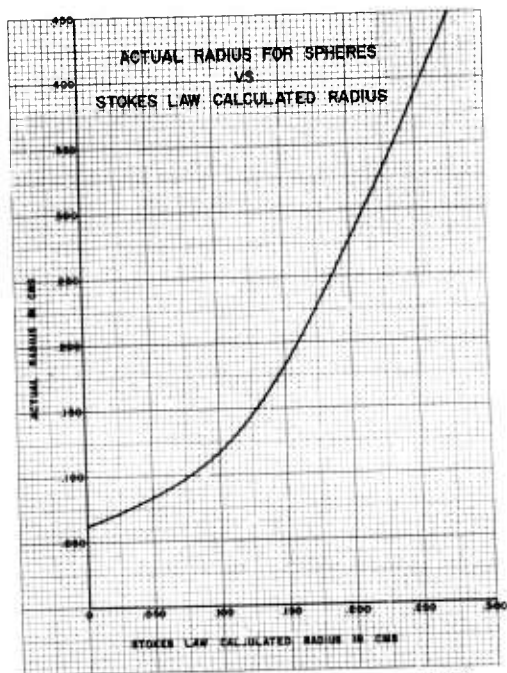
$$R^2 \text{ actual} = (r_{\text{Stokes}}^2)^{1 - 4.7r_{\text{Stokes}}^2} \quad \text{Equation (4)}$$

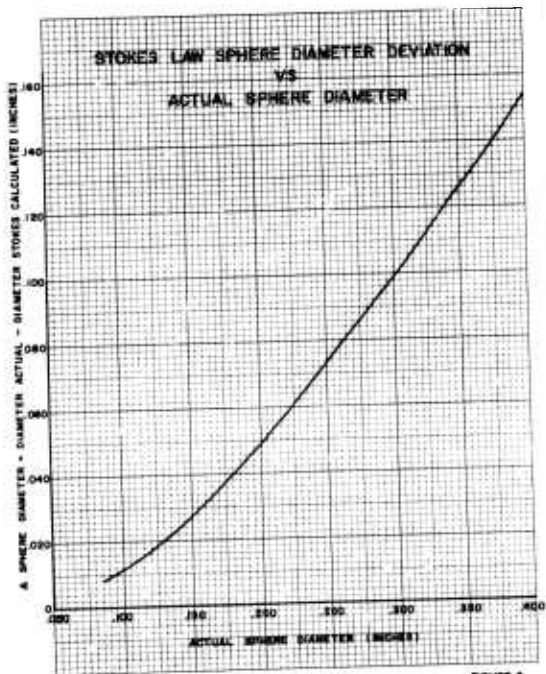
The average deviation for mean presented area using the  $R^2$  actual from equation (4) was 2.0%.

Numerical data from equation (3) and (4) for various spheres and the resulting  $\bar{A}$  deviations are to be found in Table I. Although equation (4) gave a small average deviation from the true value for spheres, correlation for other shapes could not be made and other avenues were sought.

\*See Appendix: Applicability of Stokes Law to the Measurement of Sphere Radius









Terminal velocities for uniform circular and square cross sections of steel for increasing lengths (shape ratio:  $\frac{1}{2}$  to 5) were plotted against actual  $\bar{A}$  ( $\frac{1}{2} \sum A$ ) of the particles and against their weights in Figures 4 and 5 respectively. The similarity of the latter two curves is quite striking, implying that weight and  $\bar{A}$  hold a close relation to length in its effect on terminal velocity for a uniform cross section of varying length. This might be expected, since for a uniform cross section particle, weight is directly proportional to length and  $\bar{A}$  is more directly a function of length as the lateral area becomes the dominant contributing factor for increasing lengths.

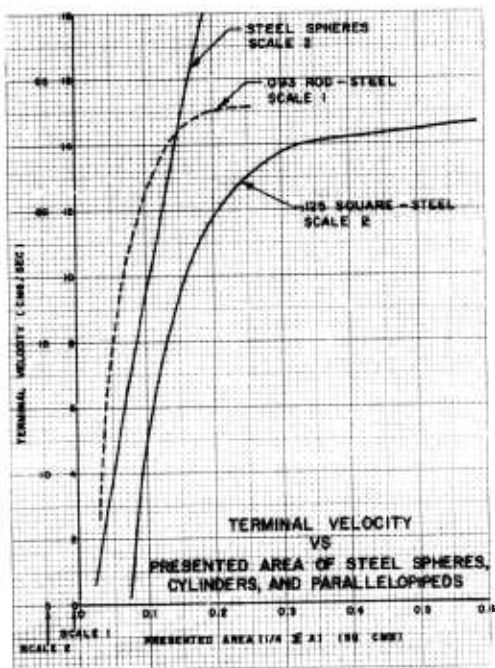
Plotting terminal velocity against shape ratio for both steel cylinders and parallelepipeds in Figure 6, note is made that terminal velocity increases sharply below a shape ratio of one, decreases sharply between the shaperatios of one to three, and that the terminal velocity approaches a constant for shape ratio beyond three.

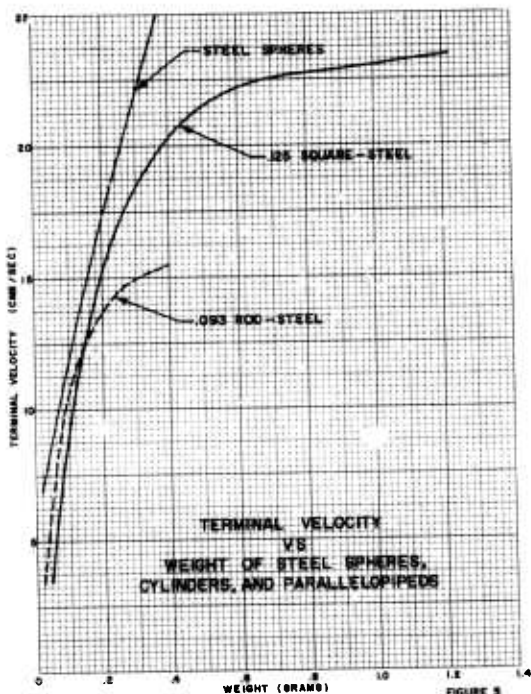
In attempting to establish an empirical expression for  $\bar{A}$  the following was assumed:

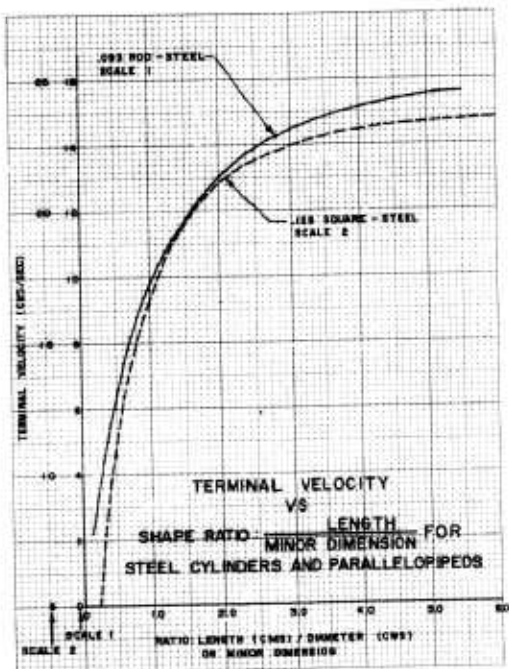
1. Weight and  $\bar{A}$  were considered as opposing factors in their effect upon particle acceleration in the fluid.
2. Terminal velocity was considered proportional to weight.
3. Terminal velocity was considered inversely proportional to  $\bar{A}$ .
4. From the above considerations, the expression

$$\text{Terminal Velocity} \propto \frac{\text{Weight}}{\bar{A}}$$

was explored, and the ratio, weight to  $\bar{A}$ , was solved as a function of terminal







velocity, i.e.,  $\frac{\text{Weight}}{\bar{A}} = f(\text{Terminal velocity})$

an expression to be tested empirically.

Plotting terminal velocity in cm/sec against the ratio of weight in grams to  $\bar{A}$  in sq. cms. for the regular shaped circular and square cross sectioned steel particles in Figure No. 7, a straight line was produced with the following equation:

$$\frac{\text{Weight}}{\bar{A}} = .0758 V + .4700$$

Equation (1)

$\bar{A}$  and  $\bar{A}$  deviation % for small steel cylinders and small steel parallelopipeds were calculated using equation (1) and tabulated in Tables 2 and 3. The  $\bar{A}$  average % deviations for the steel cylinders and parallelopipeds were 3.8% and 5.4% respectively.

For steel spheres, the actual ratio of weight to  $\bar{A}$  was computed and plotted against terminal velocity on Figure No. 7. These plotted points for spheres distributed reasonably along the curve of Figure 7. The  $\bar{A}$  and  $\bar{A}$  % deviations for spheres were calculated using equation (1) and tabulated in Table 1.  $\bar{A}$  average deviation % for spheres was 5.5%.

Steel shell fragments, previously measured for  $\bar{A}$  by B.R.L., were dropped in the viscous fluid and their terminal velocities were computed.  $\bar{A}$  for these fragments was calculated using equation (1) and tabulated in Table 4. The  $\bar{A}$  average deviation % from the B.R.L. values was 4.6%.

Uniform circular cross sectioned brass particles were tested for terminal velocity, and  $\bar{A}$  was calculated using equation (1) and tabulated in Table 5. The  $\bar{A}$  average deviation % was 2.6%.

Uniform circular cross sectioned aluminum particles were tested for terminal velocity and  $\bar{A}$  was calculated using equation (1) and tabulated in



TERMINAL VELOCITY IN A VISCOUS FLUID  
FOR STEEL FRAGMENTS VS  
RATIO:  $\frac{\text{WEIGHT}}{\text{MEAN PRESENTED AREA}}$

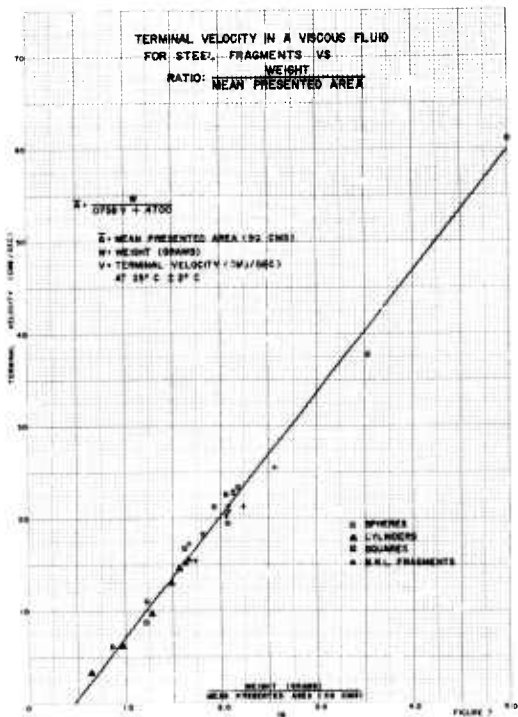


FIGURE 1

TABLE 2  
Mean Pressures Area of Small Cylinders of Steel  
Measured by Terminal Velocity in Viscous Fluid

Length inches	Length cm.	Weight grams	Weight grams	Weight grams	Velocity cm./sec.	Surface Area sq. cm.	Actual Area sq. cm.	Weight in cm. sq. cm. Ratio -Actual	Weight in cm. sq. cm. Ratio -Actual	Computed X	Deviation %	Deviation %
ratio												
5.2	4.86	1.184	.4020		15.5	.08	.12	1.66	1.55	.244	0.2	0.8
4.00	.374	.946	.297		15.1	.090	.108	1.63	1.52	.199	0.01	0.5
3.01	.221	.712	.2432		14.5	.016	.154	1.57	1.57	.154	0	0
2.01	.1869	.475	.1637		13.4	.04	.110	1.4	1.45	.113	0.03	0.7
1.0	.935	.38	.044		4.70	.244	.060	1.28	1.20	.070	0.04	0.1
0.50	.471	.112	.0420		.050	.171	.043	.975	.93	.055	0.02	0.4
0.53	.236	.060	.021		3.41	.132	.033	.638	.72	.029	0.004	0.1
Additional Data:												
Sore diameter for all cylinders = .93 in.												
Velocity was reduced to .57 in. distance												
Viscous fluid - low viscosity - 20 fluid, 20 centistokes @ 25°C												
Inlet Temperature - 25.0 ± .05												
Velocity measured 11 July 1958												
X = mean pressure area												

TABLE 3  
Mean Pressures Area of Small Square Cross Section Paraffinplate







Table 5. As seen in Table 5, the  $\bar{A}$  average deviation % was extremely high, 33.4% for these aluminum particles indicating that aluminum fragments do not follow the empirical constants in equation (1). The ratio of weight to actual  $\bar{A}$  for the aluminum particles was re-computed and plotted against terminal velocity in Figure 8. The plot gave a straight line with the following equation:

$$\frac{\text{Weight}}{\bar{A}} = .0916 V + .1538 \quad \text{Equation (5)}$$

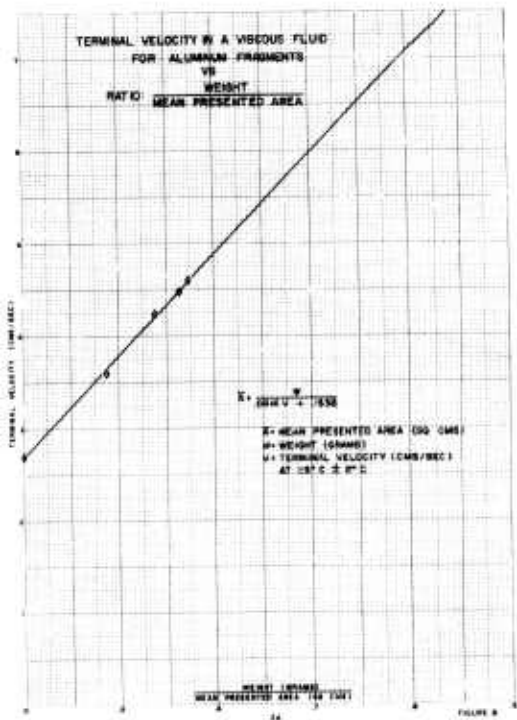
$\bar{A}$  was calculated using equation (5) and tabulated in Table 5.  $\bar{A}$  average deviation % was 0.4%.

Note is made that reasonable results were achieved using the constants in equation (1) for steel, copper and brass. The densities of the latter three metals range from 7.6 to 8.9 gms/cm<sup>3</sup>. However, for aluminum with a density of 2.69 gms/cm<sup>3</sup>, a significant departure from the 7.6 - 8.9 density range, another set of constants,  $K_1$  and  $K_2$ , had to be developed, as shown in equation (5).

In using the method of this report for measuring  $\bar{A}$  of irregular fragments below 30 grains in weight, the advantages are as follows:

1. Short time per fragment measurement.
2. No lower limit for fragment weight or mean presented area.
3. No complex instrumentation.
4. No substantial instrument cost.
5. No involved techniques.
6. Low space requirement.

In actual operation, the weight to presented area ratio can be picked off an enlarged graph or table for any particular terminal velocity.



## APPENDIX

### APPLICABILITY OF STOKES LAW TO THE MEASUREMENT OF SPHERE RADIUS

The resisting force on a sphere of radius  $r$  moving through a medium of viscosity  $\eta$  with constant velocity  $v$  was expressed by Stokes as follows:

$$F = 6\pi\eta r v \quad (A)$$

For a free falling sphere, the resisting force is equal to the sphere weight minus the fluid buoyant force, and, if  $d_1$  and  $d_2$  are sphere and fluid densities respectively, equation (A) becomes

$$\begin{aligned} M_{(\text{sphere})} g - M_{(\text{displaced fluid})} g &= 6\pi\eta r v \\ \frac{1}{3}\pi r^3 d_1 g - \frac{1}{3}\pi r^3 d_2 g &= 6\pi\eta r v \\ v &= \frac{\frac{1}{3}\pi r^3 g (d_1 - d_2)}{6\pi\eta r} = \frac{r^2 g (d_1 - d_2)}{9\eta} \\ r &= \sqrt{\frac{9\eta v}{2g(d_1 - d_2)}} \quad (B) \end{aligned}$$

Mr. B. Fairbanks, in his initial attempt at measuring mean presented area of spheres, tried to use the Stokes equation (B) and, getting no correlation, he developed the empirical expression reported in Instrumentation Report No. TR 380-58/1 in the "References."

The writer reported the results of using correction factors for Stokes law in the "Discussion" of this report and the deviation, between measured and Stokes law calculated sphere diameters versus actual sphere diameter, in Figure 3. From Figure 3, it can be seen that the deviation is approaching zero but is still appreciable for steel spheres below a weight of one grain as shown in the table below for some actual measurements:



Sphere Diam. in inches	.0937	.1562	.2500	.375
Sphere Stokes Diam. Deviation %	10.7	19.3	29.3	37.0
Sphere Weight in grains	.8441	3.889	17.13	54.32

At this point note is made of comments by others on the applicability of Stokes law as follows:

1. Elementary Mechanics of Fluids by Hunter House, 1946, Picatinny Library No. QA911 R

a. Page 158, middle of first paragraph: "Although its derivation is beyond the scope of this book, the expression for the longitudinal force  $F$  exerted by a slowly moving viscous fluid upon a small sphere, known as the equation of Stokes, is of interest at this point;

$$F = 3\pi D \eta v$$

This equation finds particular application to the fall of relatively small bodies through fluids of relatively high viscosity, - - -"

b. Page 244, first paragraph: "Resistance diagram for bodies of revolution. As indicated in Figure 125, a wealth of experimental data is at hand for the drag coefficient of spheres over a very great Reynolds-number range. At low values of  $R$  (i.e., in the zone of deformation drag) the measurements are seen to follow the straight line  $C = 24/R$ , which may be shown to correspond to the equation of Stokes Eq. (122) by the following operation:

$$F = 3\pi D \eta v \times \frac{8 D \rho v}{8 D \rho v} = \frac{24 \eta}{\rho D} \frac{\pi D^2}{4} \frac{v^2}{2} = \frac{24}{R} A \frac{\rho v^2}{2}$$

The experimental points begin to deviate from this line as soon as the accelerative effects, ignored by Stokes, begin to become appreciable; a Reynolds number slightly less than unity evidently marks the approximate limit of deformation drag, beyond which the Stokes equation is no longer applicable.

With increasing values of  $R$  the zone of appreciable viscous deformation becomes restricted more and more to the immediate boundary vicinity; at the same time, however, accelerative effects become more pronounced, and separation takes place in the zone of deceleration at the rear. By the time a Reynolds number of about  $2 \times 10^4$  is reached, the viscous shear at the boundary has become so insignificant in comparison with the pressure reduction in the zone of discontinuity that the drag coefficient no longer varies perceptibly with the Reynolds number; this condition corresponds to the pressure distribution shown in Figure 120b."

Please note that for steel spheres used, Reynolds numbers ranged from 1.04 to 28.1.

2. Fluid Mechanics by Ruseel A. Dodge and Milton J. Thomson, 1937, Picatinny Library No. QA901 D6

a. Page 175 & 176: "Experimental data on the resistance of spheres will be discussed in detail in Chap. XII, but at this point it may be mentioned that Stokes law holds only for a very restricted range of conditions. In the case of ordinary fluids, such as water and air, the size of the sphere must be so small as to be practically microscopic in character, while with larger spheres, either the fluid must be extremely viscous or the velocity must be very low. These latter cases are often referred to as 'creeping' motions.

In spite of these restrictions Stokes' law has not been without its practical applications. For example, it forms the basis for one method of measuring viscosity and has also been used to advantage in investigating the settling out of material suspended in liquids and in solving problems in diffusion."

b. Page 337: "Direct comparisons of the drag coefficients of bodies of revolution of different sections are difficult to make because of the variation of these coefficients with Reynolds' number. The most exhaustive studies in this connection have been made on spheres and the results of a large number of such investigations are shown in Figure 222. The extremely low values of  $N_r$  correspond to the viscous type of flow in which Stokes' law is valid. This solution as given by Eq. (11),  $C_d = 24/\eta_r$ , is also included in Figure 222, and it appears that this equation agrees with the experimental data only for values of  $N_r$  up to about 0.4. For higher values of  $N_r$  the inertia forces become more important and the drag coefficient decreases less rapidly with the Reynolds' number, approaching a practically constant value in the range from  $10^3$  to  $10^5$ ." (Figure 222 is reproduced on the next page).

In fluid flow around a sphere, there are inertia forces and viscous forces involved. For a low Reynolds number, the viscous forces are large compared to the inertia of the fluid particles. Stokes law solution for the drag of a sphere is based on this type of flow and breaks down when the inertia forces begin to predominate. This occurs for a Reynolds number of 0.4. Experimentally, six 1 lead shot spheres, .0543" and .0385" diameter, were checked for terminal velocity in the Dow-Corning 200 silicone fluid at  $25 \pm 2^\circ\text{C}$ . The resultant Stokes calculated diameter deviations were 0.8% and 2.5% - much smaller deviation percentages than for the previously mentioned larger steel balls.

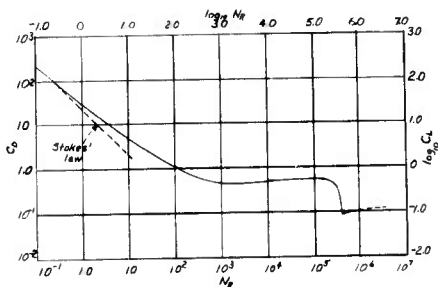


Fig. 222-Variation of drag coefficient of a sphere with Reynolds' number. (F. Eisner, Dse Widerstandsproblem, Proc. Third Int. Cong. App. Mech. (Stockholm), 1931.)

#### REFERENCES

1. Electro-Optic Icosahedron Gage - by W. R. Porter, J. L. Machamer, W. O. Ewing, Sept. 1953, B.R.L. Report No. 677, Aberdeen Proving Ground, Md.
2. Fragment Contour Projector and the Presentation Areas of Bomb and Shell Fragments - by M. R. Simpson and A. V. Buehkovitch, Nov. 1944, B.R.L. Report No. 501, Aberdeen Proving Ground, Md.
3. Fluid Mechanics - by R. C. Binder, 1955. Prentice-Hall, Inc., Englewood Cliffs, N. J.
4. Numerical Mathematical Analysis - by J. B. Scarborough, 1930, Baltimore: The Johns Hopkins Press.
5. Mathematics for Science and Engineering by Phillip L. Alger, 1957, New York: McGraw Hill Book Co., Inc.
6. Determining the Presented Area of a Fragment from its Terminal Velocity in a Grease Column - by Bernard Fairbanks, 12 June 1958. Instrumentation Report No. TR 380-58/1 Technical Service Laboratory, Feltman Research and Engineering Laboratory, Picatinny Arsenal, Dover, N. J.
7. Fluid Mechanics for Engineers - by P. S. Barna, M.E., A.F.R.Ae.S. 1957, London: Butterworths Scientific Publications.
8. Elementary Mechanics of Fluids by Hunter Rouse, 1946, New York: John Wiley & Sons, Inc.
9. Fluid Mechanics by Russell A. Dodge and Milton J. Thompson, 1917, New York: McGraw-Hill Book Co., Inc.